Chapter 4

Dual-receptor targeted chitosan-alginate nanoparticles of cabazitaxel

4. Dual-receptor targeted chitosan-alginate (CSA-NPs) nanoparticles of cabazitaxel (CZT)

4.1 Objective

The objective of this research was to develop CZT-loaded, dual-receptor (folate and EGFR) targeted CSA-NPs and to evaluate their physicochemical properties, such as shape, particle size, and zeta-potential, *in-vitro* cytotoxicity against A-549 cells, *in-vivo* pharmacokinetics, histopathology, and anticancer efficacy in B(a)P induced lung cancer mice.

4.2 Plan of study

- Preparation and characterization of chitosan-folate conjugate
- Preparation of CZT loaded dual receptor targeted CSA-NPs using solvent evaporation combined with ionic cross-linking method
- Physicochemical and *in-vitro* evaluation of dual receptor targeted CSA-NPs
- Particle size, polydispersity index and zeta potential by DLS
- Electron microscopy (SEM, TEM & AFM)
- Crystallographic studies by XRD
- Surface chemistry by XPS
- Determination of entrapment efficiency
- *In-vitro* drug release studies
- *In-vitro* cellular uptake study on A-549 cells
- *In-vitro* cytotoxicity study on A-549 cells
- *In-vivo p*harmacokinetic and histopathology studies in Wistar rats
- Anticancer efficacy studies on B(a)P induced lung cancer mice model

4.3. Material

Cabazitaxel (CZT) of the ultrapure grade was a kind of gift sample from Dr Reddy's Laboratories, Hyderabad, India. Chitosan (Molecular weight~1.5 kDa, Degree of deacetylation ≥90%), Sodium alginate LV extrapure (viscosity~10 cps, 30 mesh), succinic anhydride and EDC (1-Ethyl-3-(3-dimethylaminopropyl) carbodiimide) were procured from the Sisco Research Laboratory Pvt. Ltd (SRL) India. Folic acid, cetuximab and NHS (N-hydroxy succinimide) were provided by the Sigma-Aldrich, St. Louis, MO, USA. 4-dimethylaminopyridine (DMAP) was purchased from the Spectrochem Pvt. Ltd Mumbai (India). TPGS (D-alpha-tocopheryl-polyethyleneglycol-1000-succinate) was received as a gift sample by Antares Health Products, Inc. Dialysis membrane (Spectra/Por6®) of molecular weight 1 KDa was purchased from Spectrum Laboratories Inc., Rancho Dominguez, CA, U.S.A. The National Centre for Cell Science (NCCS) Pune, India, provided the SIRC rabbit cornea and A-549 lung cancer cell lines. MTT (3-(4,5-dimethylthiazol-2-yl)-2,5-diphenyltetrazolium bromide) were purchased from Thermo Fisher Scientific, Mumbai, India. Fetal bovine serum (EU Approved), phosphate buffer saline 10X, paraformaldehyde solution (4%), antibiotics solution 100X liquid, Dulbecco's modified Eagle's medium (DMEM) high glucose and DAPI dihydrochloride were purchased from HIMEDIA laboratories. All other reagents and substances used in the study were analytical grade and thoroughly purified.

4.4. Methods

4.4.1. Optimization of the mixture of sodium-TPP and sodium-alginate

To synthesize the CSA-NPs, an aqueous mixture of sodium-TPP and sodium-alginate was used as the crosslinking agent [191], and their combination was optimized based on the desired output such as particle size, polydispersity index (PDI) and entrapment

efficiency. Total of six runs were performed at different combinations of Na-TPP and Na-alginate while keeping their combinations constant i.e., 3 mg. As mentioned in **Table 4.1**, the required quantity of Na-TPP and Na-alginate were dissolved in the 500 µL of distilled water separately and both solutions were mixed. All of the formulations were prepared as the method described previously by using the different combinations of sodium-TPP and sodium-alginate as a cross-linking agent [188] and a combination that produced the nanoparticles with the desired particle size, PDI and entrapment efficiency was selected.

Table 4.1. Optimization of the CZT loaded CSA-NPs with different amount of the crosslinkers (sodium TPP and sodium alginate)

Formulation code	CZT (mg)	CS (mg)	TPGS (mg)	Sodium-TPP (mg)	Sodium-alginate (mg)	Particle size (nm)	PDI	Entrapment efficiency (%)
F1	3	30	20	2.75	0.25	178.6 ± 2.7	0.367 ± 0.037	74.3 ± 3.2
F2	**3**	**30**	**20**	**2.50**	**0.50**	**180.5 ± 6.2**	**0.237 ± 0.004**	**72.9 ± 4.1**
F3	3	30	20	2.25	0.75	189.7 ± 5.0	0.475 ± 0.013	70.4 ± 2.6
F4	3	30	20	2.00	1.00	275.4 ± 4.1	0.564 ± 0.037	66.2 ± 2.1
F5	3	30	20	1.75	1.25	275.8 ± 8.1	0.488 ± 0.020	65.1 ± 4.5
F6	3	30	20	1.50	1.50	315.0 ±15.4	0.411± 0.049	64.8 ± 3.9

4.4.2. Preparation of CZT/ Coumarin-6 (C6) loaded CSA-NPs

The previously reported method for the preparation of chitosan-alginate nanoparticles was used with slight modification for the preparation of CZT-CSA-NPs, CZT-CSA-F-NPs, CZT-CSA-CTXmab-NPs and CZT-CSA-F-CTXmab-NPs [125,192,193].

Concisely, CS and CS-F in the required ratio as mentioned in **Table 4.2**, were solubilized in the aqueous solution of the acetic acid (1 % v/v). The aqueous NaOH solution was used to maintain pH 6.0. Simultaneously, 1mL of aqueous solution of TPGS or TPGS-COOH (20 mg/mL) was added. Subsequently, 1 mL of CZT in chloroform (3 mg/mL) was added to the above solution and both the immiscible liquids were sonicated for 5 min using an ultrasonic probe sonicator (Hielscher UP200H, Germany). Afterwards, the obtained milky emulsion was stirred overnight to achieve complete evaporation of the chloroform. The optimized mixture of the Na-TPP and Na-alginate **(Table 4.2)** was added dropwise to the chitosan solution at a very low rate and kept stirring for 1 h. To accomplish post-conjugation with CTXmab, carbodiimide crosslinkers, EDC: NHS in a 1:5 molar ratio to TPGS-COOH, were added to the aforementioned carboxylic functionalized CSA-NPs and agitated for 30 min. Afterwards, 2.5 mg of the CTXmab was added to the CSA-NPs and kept on stirring for 30 min. Subsequently, the formulation was dialyzed for 1 h in the saturated solution of CZT employing a 1 KDa dialysis membrane. Afterwards, the nanoparticle dispersion was centrifugated to remove larger particles at 1000 rpm for 10 min before being filtered through a 0.22 μm membrane filter. For the cellular-uptake characterization, a set of C6 loaded non-targeted (C6-CSA-NPs), folate targeted (C6-CSA-F-NPs), EGFR targeted (C6-CSA-CTXmab-NPs), and dual-receptor targeted (C6-CSA-F-CTXmab-NPs) formulations were prepared by loading C6 (0.3 mg) instead of CZT, using the same procedure as described above.

Table 4.2. Formulation of various CSA-NPs

Batches	CS-F (mg)	Chitosan (mg)	TPGS (mg)	TPGS-COOH (mg)	CTXmab (mg)	CZT (mg)	Sodium -TPP (mg)	Sodium-Alginate (mg)
CZT- CSA-NPs	-	30	20	-	-	3	2.5	0.5
CZT-CSA-F-NPs	9	21	20	-	-	3	2.5	0.5
CZT-CSA-CTXmab-NPs	-	30	10	10	2.5	3	2.5	0.5
CZT-CSA-F-CTXmab-NPs	9	21	10	10	2.5	3	2.5	0.5

CZT-CSA-NPs: CZT loaded CSA-NPs
CZT-CSA-F-NPs: CZT loaded folate receptor targeted CSA-NPs
CZT-CSA-CTXmab-NPs: CZT loaded EGFR targeted CSA-NPs
CZT-CSA-CTXmab-F-NPs: CZT loaded EGFR and folate targeted CSA-NPs

4.4.2. Characterization of nanoparticles

4.4.2.1. Surface charge, particle size, and polydispersity

The Malvern Zetasizer (Nanoseries) was used to evaluate the surface charge, hydrodynamic particle size, and PDI of CSA-NPs at 25 °C using the dynamic light scattering principle [194].

4.4.2.2. Electron microscopic evaluation of CSA-NPs

4.4.2.2.1. Transmission electron microscopy (TEM) analysis

The size, shape and morphology of prepared CSA-NPs at the nanoscale was investigated using TEM analysis (Tecnai G2 20 Twin). The samples were prepared by the drop-casting method without employing staining. The CSA-NPs were sonicated for 5 min after being diluted in distilled water and a drop was casted on the carbon-coated copper TEM grid (400 Mesh) and dried overnight before analysis [195].

4.4.2.2.2. Scanning electron microscopy (SEM analysis)

Scanning electron microscope was used to examine the surface morphology of CSA-NPs (Carl Zeiss Microscopy Ltd). The images were captured with a magnification of 50 KX and a voltage of 20 kV. The samples were diluted with ultrapure water and placed one drop of sample on the coverslips, which were further dried for 24 h at 40 °C. Prior to SEM examination, the produced samples were subjected for a carbon coating [196].

4.4.2.2.3. Atomic force microscopy (AFM) analysis

The shape, morphology and roughness of the CSA-NPs was analyzed by AFM analysis (NT-MDT Service & Logistics Ltd). The samples were prepared after dilution with ultrapure water. After sonication for 10 min, a drop of prepared samples was kept on the microscope slide (1 x 1 cm) and dried for 24 h. To obtain roughness profile and 2-D/ 3-D AFM images of the CSA-NPs, the NOVA, NT-MDT software was used for image processing [197].

4.4.2.3. Surface chemistry

X-ray photoelectron spectroscopy (XPS) (Thermo Scientific K-Alpha XPS System) was used to characterize the surface chemical analysis of prepared nanoparticles at binding energies ranging from 100 to 700 eV. The specimens were casted by dropping the CSA-NPs on a glass slide (1 x 1 cm) and kept for drying overnight, in a vacuum dryer before analysis [198].

4.4.2.4. Degree of conjugation

4.4.2.4.1. Folic acid content

The folate content in the folate targeted formulations (CZT-CSA-F-NPs and CZT-CSA-F-CTXmab-NPs) was determined by using a multi-mode microplate reader (Molecular Devices, USA). Concisely, 200 µL of the respective formulations were freeze-dried and

dissolved in the DMSO: DCM (4:1). After vortexing for 6 h, samples were centrifuged and the filtered supernatant was used for the UV-Visible analysis. The folate content was determined by plotting the calibration curve of the folic acid at λ max = 364 nm, and the total folic acid content present in the folate conjugated CSA-NPs was determined. The percent folic acid content was computed by the given formula [171,199].

$$Degree\ of\ folate\ conjugation\ (\%) = \frac{Folate\ content\ determined\ within\ NPs}{Total\ folate\ content\ used\ in\ NPs} * 100$$

4.4.2.4.2. CTXmab content

Bradford assay was used to determine the CTXmab content on the surface of CZT-CSA-CTXmab-NPs and CZT-CSA-F-CTXmab-NPs. The PBS (pH 7.4) was used as a negative control. Briefly, 40 µL of respective formulations were added to a 96-well plate and subsequently, 200 µL of Bradford reagent was added and incubated for 5 min in darkness. Afterwards, the samples were analyzed using multi-mode microplate reader (Molecular Devices, USA), and the concentration of CTXmab was determined using the standard curve of BSA [200].

$$Degree\ of\ CTXmab\ conjugation\ (\%) = \frac{CTXmab\ content\ determined\ in\ NPs}{CTXmab\ content\ in\ std.\ solution} * 100$$

4.4.2.5. Determination of entrapment efficiency

HPLC (LC-20AR, with PDA detector, Shimadzu, Japan), was used to measure the entrapment efficiency of prepared CSA-NPs. Concisely, 200 µL of the CSA-NPs (equivalent to 60 µg of CZT) were transferred to a spherical flask and dried using a rotary evaporator. Subsequently, the dried residue of the nanoparticles was treated with methanol and vortexed overnight. The resulting solution was centrifuged at 10,000 rpm

for 10 min and the supernatant was dried using a rotary evaporator after filtration by a membrane filter (0.22 μm). A methanol/water system (75:25 ratio) was employed as the mobile phase in the experiment. The dried content of CZT was solubilized in 1 mL of mobile phase and vortexed for 10 min. The samples were then filtered using a 0.22 μm membrane filter before adding to the HPLC vials. The CZT standard curve was prepared in the mobile phase and the graph between the standard concentrations versus the peak area was plotted. The entrapment efficiency of CSA-NPs was calculated [201,202]. Furthermore, the entrapment efficiency of C6 in C6-loaded CSA-NPs was determined by using a multi-mode microplate reader (Molecular devices, USA). Briefly, 30 μL of C6-loaded CSA-NPs were dried using a rotary evaporator. The dried content was dispersed in 70 μL of methanol, and vortexed for 24 h. The resulting solution was diluted up to 1000 μL with water and filtered through a 0.22 μm membrane filter. Concisely, 200 μL of the filtered sample was placed in the 96-well opaque plate and the absorbance was recorded at the fluorescent mode at an excitation wavelength of 462 nm and an emission wavelength of 502 nm. The entrapment efficiency was calculated by the formula as stated below [125,202].

$$Entrapment\ efficiency\ (\%) = \frac{CZT\ amount\ entrapped\ in\ NPs}{Total\ CZT\ amount\ used\ in\ the\ prepration} * 100$$

4.4.2.6. X-ray diffraction (XRD) analysis

XRD analysis of CZT, CZT-CSA-NPs, CZT-CSA-F-NPs, CZT-CSA-CTXmab-NPs and CZT-CSA-CTXmab-NPs together with Na-TPP and folic acid was performed by using Bench Top X-Ray Diffraction (BT-XRD: RIGAKU Corporation). The CZT, Na-TPP and folic acid were in powder form was used for the analysis. However, CZT loaded CSA-NPs were lyophilized for 12 h prior to the XRD analysis [182].

4.4.2.7. In-vitro evaluation

4.4.2.7.1. In-vitro release study

The dialysis bag diffusion technique was used to investigate the CZT release profile from the CSA-NPs. The CSA nanoparticle samples, which were equivalent to 300 µg of the CZT, were placed in a dialysis tube (1 KDa) and closed with the dialysis tube closures. The dialysis bag assembly was placed in a flask containing 50 mL of PBS pH 7.4 and pH 5.5 and shaken continuously at 37 ± 0.5 ℃ in a shaking water bath apparatus (Remi Cm-12 Plus, Mumbai, India). Precisely, 1 mL of the respective media was taken at the pre-scheduled time, and the same volume of fresh media was replaced. All samples were filtered through a membrane filter and vacuum dried. Subsequently, the dry CZT residue was then solubilized in 5 mL of the mobile phase and the concentration of each sample was determined by HPLC analysis. The graph was plotted between time and the percent cumulative drug release [174].

4.4.2.7.2. In-vitro cellular uptake study

The cellular uptake study of pure-C6 and C6 loaded non-targeted, folate receptor targeted, EGFR targeted, and dual-receptor targeted CSA-NPs was performed on A-549 cells by using a fluorescent microscope. Cells were plated in a 12-well plate at a density of $5x10^4$ cells per well and left to grow for 24 h. The pure-C6 and C6-loaded formulations were then diluted in complete DMEM to make 5 µg/mL concentration and incubated at 37 °C for 12 h. Afterwards the cells were washed 3 times with PBS and being fixed for 15 min with 4 % formaldehyde solution. Thereafter, the nuclei of the cells were stained with 4′,6-diamidino-2-phenylindole (DAPI) and the media was withdrawn from the wells after 15 min. Subsequently, the cells were irrigated with PBS once more. The fluorescence images of internalized nanoparticles were obtained in a comparable blue (DAPI) and green

channel (C6). Furthermore, the degree of cellular internalization of C6-loaded nanoparticles was measured by image-J software. The percentage area of green channels was detected, indicating the nanoparticle internalized in A-549 cells [200].

4.4.2.7.3. In-vitro cytotoxicity assay

The cytotoxicity analysis of CZT (control), CZT-CSA-NPs, CZT-CSA-F-NPs, CZT-CSA-CTXmab-NPs, CZT-CSA-F-CTXmab-NPs was carried out by MTT assay against A-549 and SIRC cell lines. The cells were plated in a 96-well culture plate at the density of $5x10^4$ cells each well in DMEM and incubated in CO_2 humidified incubator (5%) at 37 ºC. The used-up media was removed after 24 h, and the CSA-NPs with the required dilution in DMEM medium were treated with the cells for another 24 h. Again, the used-up media was replaced with 90 µL of the fresh medium and 10 µL of MTT solution (5 mg/mL in PBS, pH 7.4) was added and incubated for 4 h. Afterwards, the medium was aspirated without unsettling the formazan crystals. After subsequently washing and drying for 2h, 100 µL of DMSO was added and the 96-well plate was placed on a shaker. The absorbance of the samples was measured at 570 nm using a microplate reader [203]. Cell viability (%) was calculated as a percentage of the ratio of the absorbance of treated and untreated cells. The following formula was used to calculate the percentage cell viability [204].

$$\text{Cell viability (\%)} = \frac{\text{Absorbance of treated cells}}{\text{Absorbance of control cells}} \text{ X } 100$$

4.4.2.8. In-vivo evaluation

4.4.2.8.1. Pharmacokinetic analysis

Wistar rats (healthy, male and female) weighing 150–200 g and aged 4–5 weeks were housed in a regulated temperature and humidity conditions. The animals were kept in a 12-h light/dark cycle for 15 days at a temperature of 20–26 °C and relative humidity of

30–70 %. The rats were randomly divided into six groups (n = 3). The negative control group received the saline by intravenous (i.v.) (tail vein) route, while the positive control group received CZT (control) at a 3.5 mg/kg dose. The other four groups (CZT-CSA-NPs, CZT-CSA-F-NPs, CZT-CSA-CTXmab-NPs and CZT-CSA-F-CTXmab-NPs) were administered with the respective nanoparticles at the equivalent dose of CZT. Approximately, 500 µL of the blood was collected through the orbital venous plexus at the pre-scheduled time points (0.5, 1, 2, 4, 8, 12, 24, and 48 h) and transferred in the Eppendorf tubes containing sodium citrate (3.8 % w/v) and vortexed for 10 min. Subsequently, the vials were centrifuged for 10 min at 6000 rpm. The CZT content was extracted from plasma samples using the protein precipitation method, which was then analyzed using the RP-HPLC method. Acetonitrile and methanol (50:50) were used as the precipitating solvents. Briefly, 300 µL of the prepared precipitating solvent mixture was added to 140 µL of the separated plasma and vortexed for 5 min. The samples were then centrifuged at 6000 rpm for 10 min, and the supernatant was filtered through the 0.22 µm membrane filter and used for HPLC analysis. The concentration of a drug in the plasma versus time intervals was plotted and the various pharmacokinetic metrics were computed using Kinetica 5.0 software [202].

4.4.2.8.2. Histopathology study

The Wistar rats were used in a histopathology investigation to determine the safety of dual-targeted CSA-NPs. Animals were arbitrarily divided into six groups, each with four rats. The prepared nanoparticles were administered through i.v. route via tail vein. The saline control and standard groups were administered with the saline and CZT (control), respectively. Although, the remaining animal groups 3 to 6 were administrated with CZT-CSA-NPs, CZT-CSA-F-NPs, CZT-CSA-CTXmab-NPs, and CZT-CSA-F-CTXmab-NPs

at a dose equivalent to 3.5 mg/kg of CZT control. The treatment was given three times at a three-day interval, and all the animals were euthanized on the 15th day. The vital organs of all the animals including lungs, livers, kidneys, and hearts were taken and stored in the formalin solution (10 % v/v). Afterwards, the specimen was placed in the paraffin box and sliced at a thickness of 4 µm using a microtome. After that, haematoxylin and eosin dyes were used to stain the sections. A light microscope was used to observe the histopathological changes and images were captured by using the Capture pro 4.1 software [187].

4.4.2.8.3. Tumour regression and survival analysis

Swiss albino mice weighing 16–20 g were used in the investigation. All the animals were housed in a regulated temperature and humidity environments with constant humidity and 12-h light/dark cycle. Randomly, the mice were divided into seven groups (n = 4). Corn-oil was employed as a vehicle to deliver B(a)P orally by using an oral gavage. The calculated amount of B(a)P was dissolved in the corn-oil using a bath-sonicator. The control group was given an equivalent amount of corn oil for 16 weeks, while the cancer model control group and other groups 3–7 were given B(a)P-corn oil solution at 50 mg/kg. This resulted B(a)P-corn oil solution was administered twice a week up to four weeks. After the second week of B(a)P exposure, groups 3 to 7 were given CZT (marketed formulation), CZT-CSA-NPs, CZT-CSA-F-NPs, CZT-CSA-CTXmab-NPs, and CZT-CSA-F-CTXmab-NPs intravenously twice weekly through tail vein at a dose of 6.5 mg/kg equivalent to CZT control. Afterwards, the animals were sacrificed, and the lungs were collected, preserved in formalin solution (10% v/v), and subjected to histopathological analysis. Haematoxylin dye gives the nuclei a blue colour, while eosin stains the pink colour to the extracellular matrix and cytoplasm. Approximately, 4 µm thick paraffin

sections were placed on individual glass slides and stained with hematoxylin and eosin (HE). The bright microscopic images were taken at 10X and the numbers of nuclei were counted in each image by using ImageJ software by separating the blue channels using the "split channels" option. The blue-channel images were then transformed into binary black-and-white images and subsequently processed to estimate the nuclei number. Throughout the study, the health condition of the animals was assessed every day, and their body weights were measured once a week. Kaplan–Meier survival analysis were used to compute the percent survival rate [164,188].

4.5. Results and discussion

4.5.1. Particle size distribution and surface charge

The physicochemical parameters of CZT/C6 loaded CSA-NPs are shown in **Table 4.3**. The CSA-NPs showed the hydrodynamic particle sizes ranging from 180 to 220 nm. The particle size of the dual receptor-targeted CSA NPs was significantly higher ($p<0.05$) than that of the non-targeted CSA-NPs, possibly due to surface modification with folic acid and CTXmab. The surface charge of CZT- CSA-NPs, CZT-CSA-F-NPs, CZT-CSA-CTXmab-NPs and CZT-CSA-CTXmab-F-NPs was 31.8 ± 2.3 mV, 30.0 ± 2.1 mV, 29.1 ± 1.6 mV and 25.5 ± 1.9 mV respectively. All CSA-NPs elicited zeta reports in the range of +25 mV to +32 mV, revealing that they were extremely stable. As a consequence of the dominating anionic groups of folic acid and CTXmab, the surface charge of dual receptor-targeted CSA-NPs is slightly lower ($p < 0.05$) than that of non-targeted CSA-NPs, implying the successful surface modification of CSA-NPs with dual ligands.

Table 3. Particle size distribution; surface charge, entrapment efficiency and IC_{50} values of CZT and C6 loaded CSA-NPs.

Batches	Particle Size (mean ± SD*) nm	Polydispersity index (mean ± SD*)	Zeta potential (mean ± SD*) mV	Entrapment efficiency (%) (mean ± SD*)	IC_{50}Value (mean ± SD*) µg/mL
CZT-Control	-	-	-	-	15.27 ± 1.2
CZT- CSA-NPs	181.5 ± 5.1	0.269 ±0.062	31.8 ± 2.3	75.5 ± 1.9	8.11 ± 1.5
CZT-CSA-F-NPs	178.2± 12.5	0.223 ± 0.082	30.0 ± 2.1	73.6 ± 2.1	6.49 ± 0.7
CZT-CSA-CTXmab-NPs	197.2 ± 4.4	0.352 ± 0.069	29.1 ± 1.6	71.4 ± 1.7	5.33 ± 0.6
CZT-CSA-CTXmab-F-NPs	210.3 ± 7.4	0.295 ± 0.015	25.5 ± 1.9	69.9 ± 2.0	0.40 ± 0.03
C6- CSA-NPs	175.2 ± 4.5	0.241 ± 0.041	32.1 ± 1.8	76.3 ± 3.1	-
C6-CSA-F-NPs	179.2 ± 3.2	0.312 ± 0.033	30.5 ± 2.7	74.7 ± 2.8	-
C6-CSA-CTXmab-NPs	185.4 ± 4.6	0.214 ± 0.027	28.4 ± 1.8	72.4 ± 2.6	-
C6-CSA-F-CTXmab-NPs	195.4 ± 6.1	0.287 ± 0.030	24.7 ± 2.2	71.4 ± 3.2	-

CZT-Control: Clinical injection of CZT
CZT- CSA-NPs: CZT loaded CSA NPs
CZT-CSA-F-NPs CZT loaded folate targeted CSA NPs
CZT-CSA-CTXmab-NPs: CZT loaded EGFR targeted CSA NPs
CZT-CSA-F-CTXmab-NPs: CZT loaded folate and EGFR targeted CSA NPs
C6- CSA-NPs: C6 loaded CSA NPs
C6-CSA-F-NPs C6 loaded folate targeted CSA NPs
C6-CSA-CTXmab-NPs: C6 loaded EGFR targeted CSA NPs
C6-CSA-F-CTXmab-NPs: C6 loaded folate and EGFR targeted CSA NPs

4.5.2. Electron microscopic evaluation of CSA-NPs

4.5.2.1. Transmission electron microscopy (TEM) analysis

The shape, size, surface morphology, elemental analysis, and physical state of CSA-NPs were characterized using the TEM analysis. **Figure 4.1. A** displayed the TEM images of various nanoparticle formulations at the resolution of 50 nm to 100 nm. The TEM images of CZT-CSA-F-NPs, CZT-CSA-CTXmab-NPs, and CZT-CSA-F-CTXmab-NPs revealed tiny depositions on the surface that could be interpreted as conjugated targeted moieties.

4.5.2.2. Scanning electron microscopy (SEM) analysis

The surface topography and size distribution of CSA-NPs were determined using scanning electron microscopy. SEM images in **Figure 4.1. B** showed that nanoparticle formulations were monodisperse, and smooth-surfaced without visible pinholes or cracks.

4.5.2.3. Atomic force microscopy (AFM) analysis

Atomic force microscopy was used to examine the surface topography of nanoparticle formulations. As demonstrated in **Figure 4.1. C and 4.1. D**, the CSA-NPs have a spherical shape and a smooth surface with no apparent pinholes or cracks.

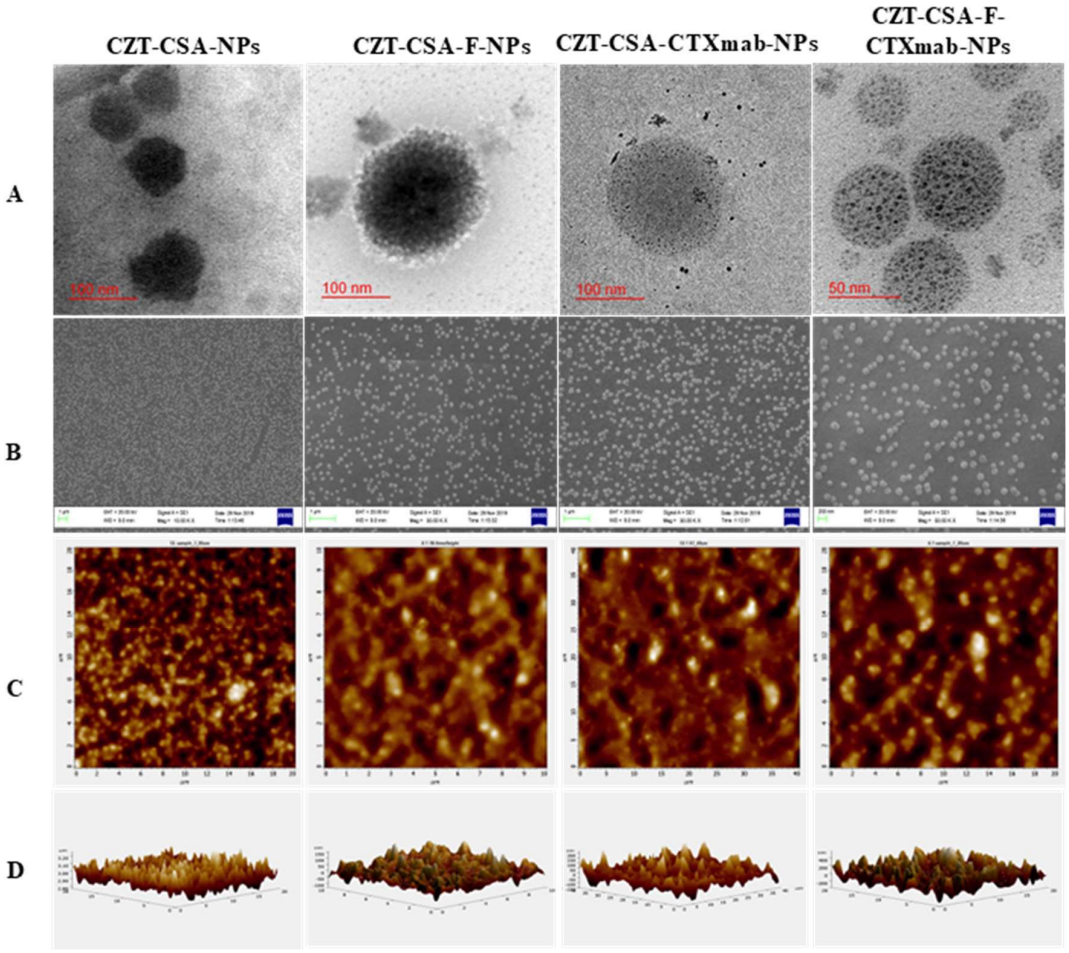

Figure 4.1. A) TEM, B) SEM, C) 2-D AFM and D) 3-D AFM images of CZT-CSA-NPs, CZT-CSA-F-NPs, CZT-CSA-CTXmab-NPs and CZT-CSA-F-CTXmab-NPs

4.5.3. Surface chemistry

XPS was used to investigate the surface chemistry of CSA-NPs. The distinctive peaks of nitrogen, carbon and oxygen were analyzed in the XPS survey of the respective nanoparticles, as shown in **Figure 4.2. A**. The peaks of N 1s, C 1s, and O 1s were observed at binding energies of 408–390, 298–280 and 545–529 eV, respectively. **Figure 4.2. A**. demonstrated the atomic percentage of nitrogen (N 1s) in the XPS spectra of CSA-NPs increased in the order of CZT-CSA-NPs < CZT-CSA-F-NPs < CZT-CSA-CTXmab-NPs < CZT-CSA-F-CTXmab-NPs. This increase in the atomic percentage of nitrogen can be associated with the significant number of nitrogen atoms in the structure of folic acid and CTXmab.

4.5.2.4. Determination of entrapment efficiency

The percent entrapment of the CZT in the CZT-CSA-NPs, CZT-CSA-F-NPs, CZT-CSA-CTXmab-NPs, CZT-CSA-F-CTXmab-NPs was 75.5 ± 1.9 %, 73.6 ± 2.1 %, 71.4 ± 1.9 % and 69.9 ± 2.0 %. The percent C6 entrapment of C6-CSA-NP, C6-CSA-F-NP, C6-CSA-CTXmab-NP, and C6-CSA-F-CTXmab-NP was 76.3 ± 3.1 %, 74.7 ± 2.8 %, 72.4 ± 2.6 % and 71.4 ± 3.2 % respectively (**Table 4.3**). For dual-receptor targeted CSA-NPs, the entrapment efficiency was somewhat lower than that of the single-receptor targeted and non-targeted CSA-NPs which can be due to the interference of the targeting ligands (folic acid and CTXmab) on the surface of nanoparticles.

4.5.2.5 Degree of conjugation

4.5.2.5.1. Folic acid

The quantity of folic acid conjugated to the CZT-CTZ-F-NPs and CZT-CSA-F-CTXmab-NPs was 68.3 ± 3.0 % and 66.6 ± 2.3 %, respectively. The presence of CTXmab on the

nanoparticle surface can justify the reduction of the folic acid fraction in dual-targeted chitosan-alginate nanoparticles.

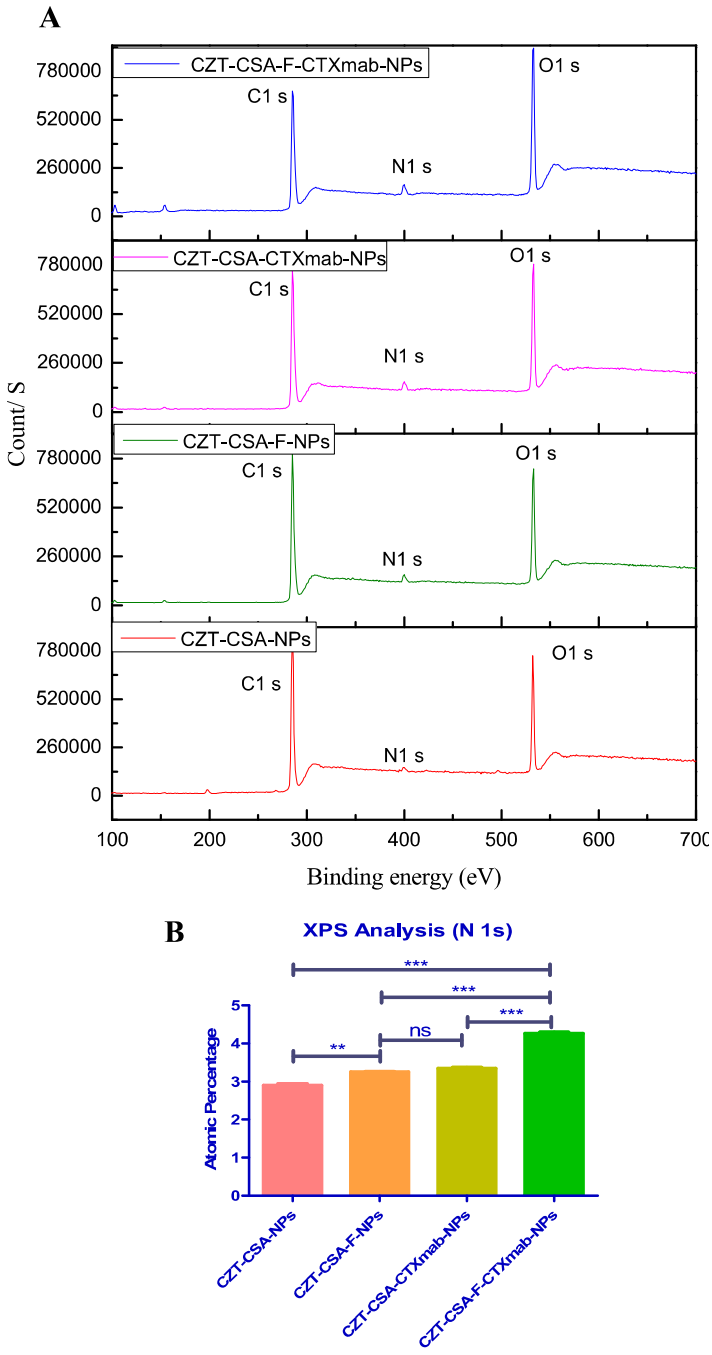

Figure 4.2. A) XPS survey of CZT loaded CSA-NPs B) Histogram showing the atomic percentage of N 1s

4.5.2.5.2 CTXmab

The degree of CTXmab conjugation on the surface of CZT-CSA-CTXmab-NPs and CZT-CSA-F-CTXmab-NPs was assessed using the Bradford assay. As per the observations, approximately 71.53 ± 4.21 % of CTXmab conjugation was achieved in a CTXmab conjugated CSA-NPs, but it was 67.32 ± 4.03 % in dual receptor-targeted CSA-NPs. The slight decrease in the CTXmab content of dual receptor-targeted CSA-NPs, might be due to the interference of folic acid, which could decrease the accessible surface area.

4.5.2.6. X-ray diffraction (XRD) analysis

The physical state of the nanoparticle formulations and also the existence of the respective targeting ligands were disclosed by XRD analysis of CZT, CZT-CSA-NPs CZT-CSA-F-NPs, CZT-CSA-CTXmab-NPs, and CZT-CSA-CTXmab-NPs (**Figure 4.3**). The XRD spectra of the CZT showed broad peaks which revealed its amorphous nature. The XRD analysis of Na-TPP and folic acid exhibited distinct sharp peaks, showing that both are in the crystalline state. The XRD spectra of CZT-CSA-NPs showed broad peaks and numerous well-defined sharp peaks at 2 θ of 32.1°, 45.9°, 56.9°, 66.6°, 75.9°, 84.5°. However, similar sharp peaks have also appeared in the XRD spectra of CZT-CSA-F-NPs at 2 θ of 31.8°, 45.5°, 56.4°, 66.3°, 75.3° and 84.4° with a lesser intensity which revealed their semi-crystalline characteristics. The Na-TPP was used to fabricate the CSA-NPs, which resulted in the formation of polyelectrolyte complexed nanoparticles. Since the distribution of chitosan, alginate, and Na-TPP in the polyelectrolyte complex is consistent throughout the nanoparticles, and some Na-TPP content may be retained on the surface of nanoparticles. Therefore, the Na-TPP may be responsible for the sharp crystalline peaks observed in the XRD spectra of the CZT-CSA-NPs and CZT-CSA-F-NPs. Contrastingly, the XRD spectra of CZT-CSA-CTXmab-NPs displayed only one

peak at 2 θ of 31.8° with a substantial reduced-intensity which can be explained by the CTXmab coating over the surface of nanoparticles. Finally, the XRD spectra of the CZT-CSA-F-CTXmab-NPs displayed no sharp peaks, which can be correlated with the presence of both the targeting ligands, i.e., folate and CTXmab. However, the peaks observed in the XRD spectra of CZT did not match with any of the formulations, indicating that the drug is successfully loaded in the formulations. Hence, the XRD analysis revealed the physical state of the CSA-NPs with the evidence of the coating with the targeting ligands [205,206].

4.5.2.7. In-vitro evaluation

4.5.2.7.1 CZT release profile

CZT release profiles from the CZT-CSA-NPs, CZT-CSA-F-NPs, CZT-CSA-CTXmab-NPs and CZT-CSA-F-CTXmab-NPs were examined in PBS pH 7.4 and pH 5.5, and the results are displayed in **Figure 4.4. A and 4.4. B**. The initial release of the CZT from the CSA-NPs follows a burst release (which could be a loading dose), followed by 72 h of constant release (keeping the desired drug concentrations constant). The t_{50} (time required for the release of 50% of the drug) of CZT control, CZT-CSA-NPs, CZT-CSA-F-NPs, CZT-CSA-CTXmab-NPs and CZT-CSA-F-CTXmab-NPs at the pH 5.5 was 0.63 h ± 0.01, 7.8 h ± 0.011, 8.3 h ± 0.012, 9.4 h ± 0.014 and 10.41 h ± 0.013 h respectively. **Figure 4.4. C** shows the t_{50} of different CSA-NPs at pH 5.5 and 7.4. The extent of CZT released from CSA-NPs was slightly higher in PBS pH 5.5 than in PBS pH 7.4, which is attributed to higher solubilization of the chitosan (used in higher quantity than alginate) in an acidic environment, implying that CZT will release more in the cancerous acidic microenvironment [207].

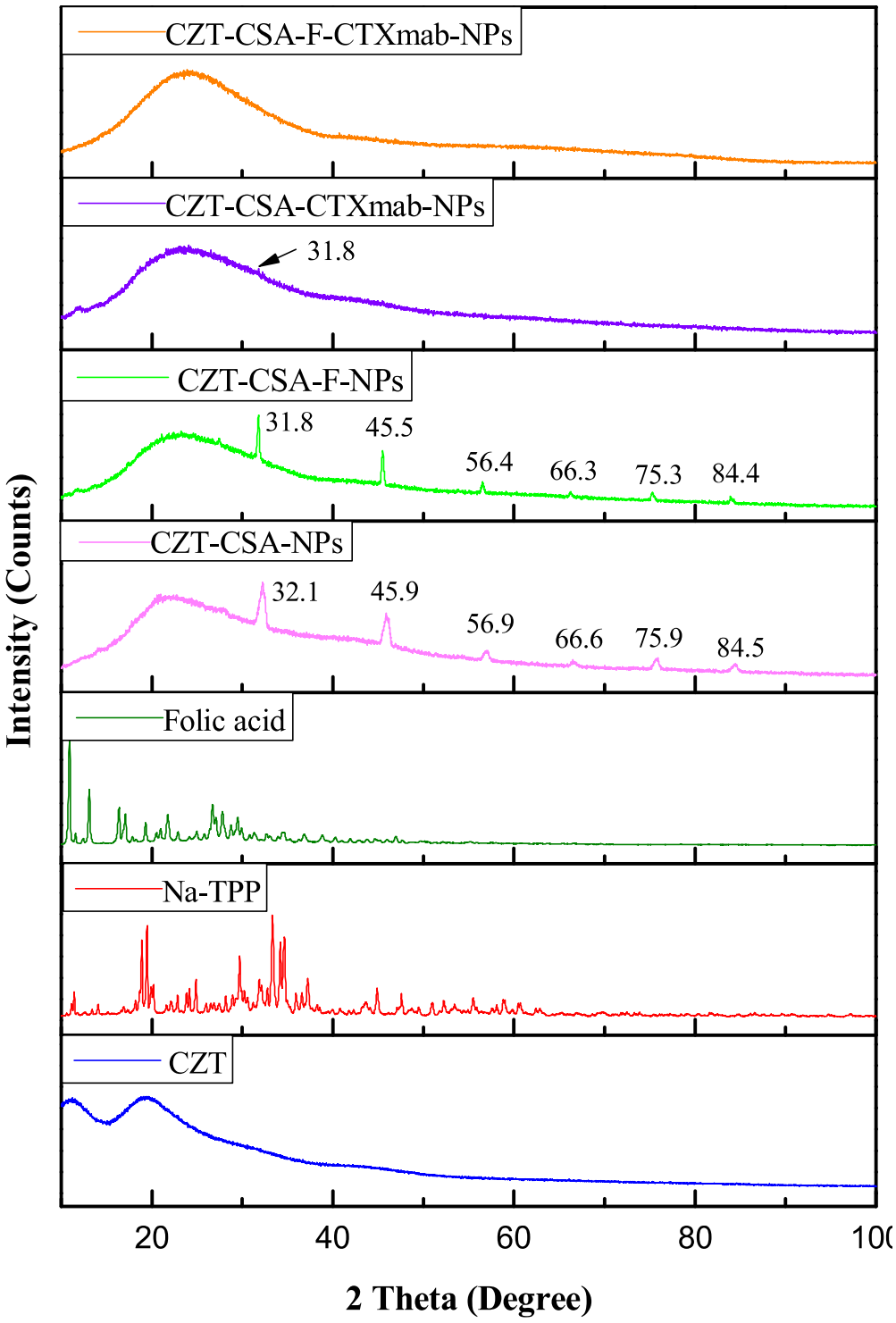

Figure 4.3. XRD spectra of CZT, CZT-CSA-NPs, CZT-CSA-F-NPs, CZT-CSA-CTXmab-NPs and CZT-CSA-CTXmab-NPs

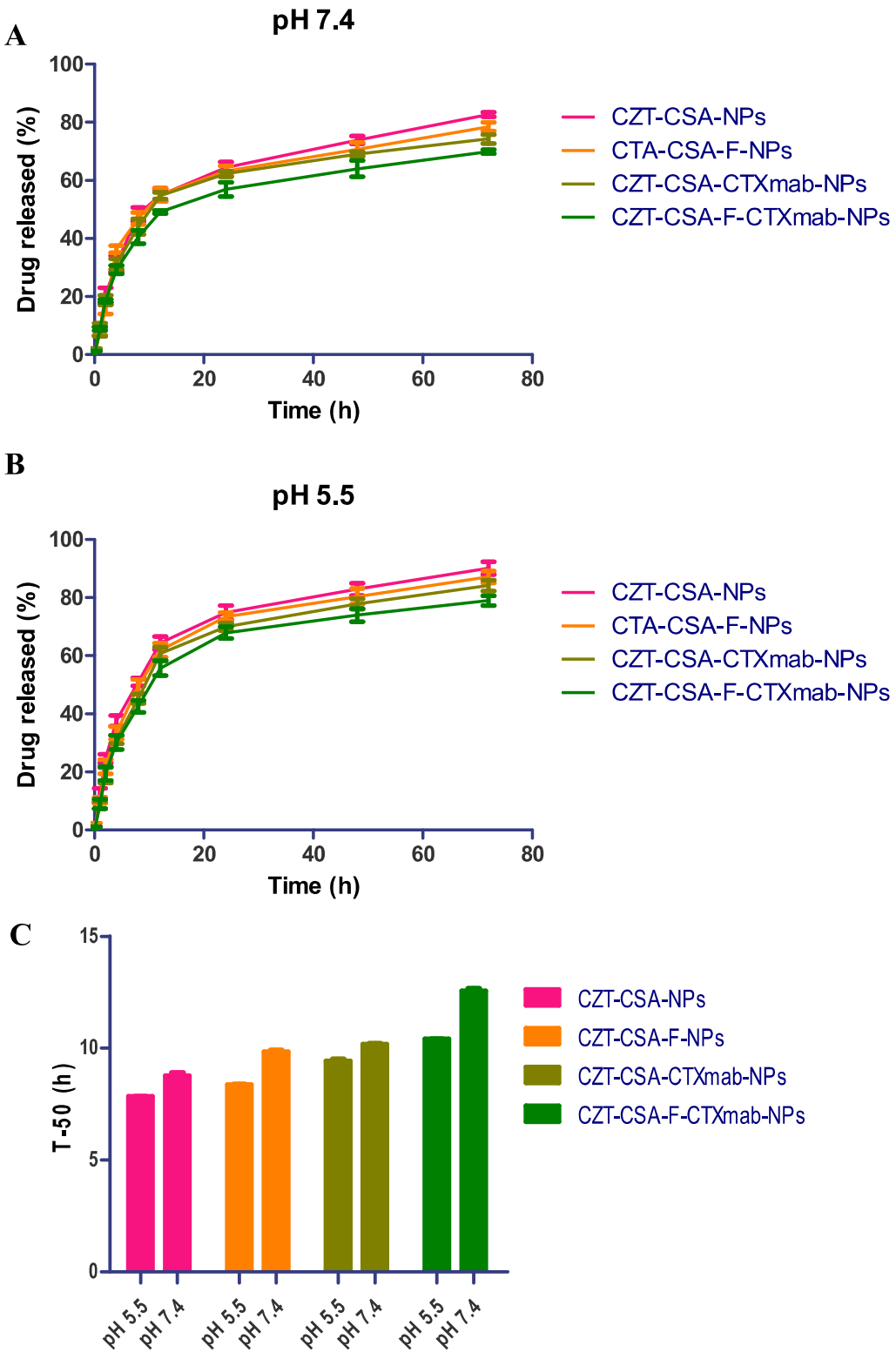

Figure 4.4. A) CZT release profile at pH 5.5, B) CZT release profile at pH 7.4, and C) t_{50} (h) of CZT loaded CSA-NPs at pH 5.5 and pH 7.4

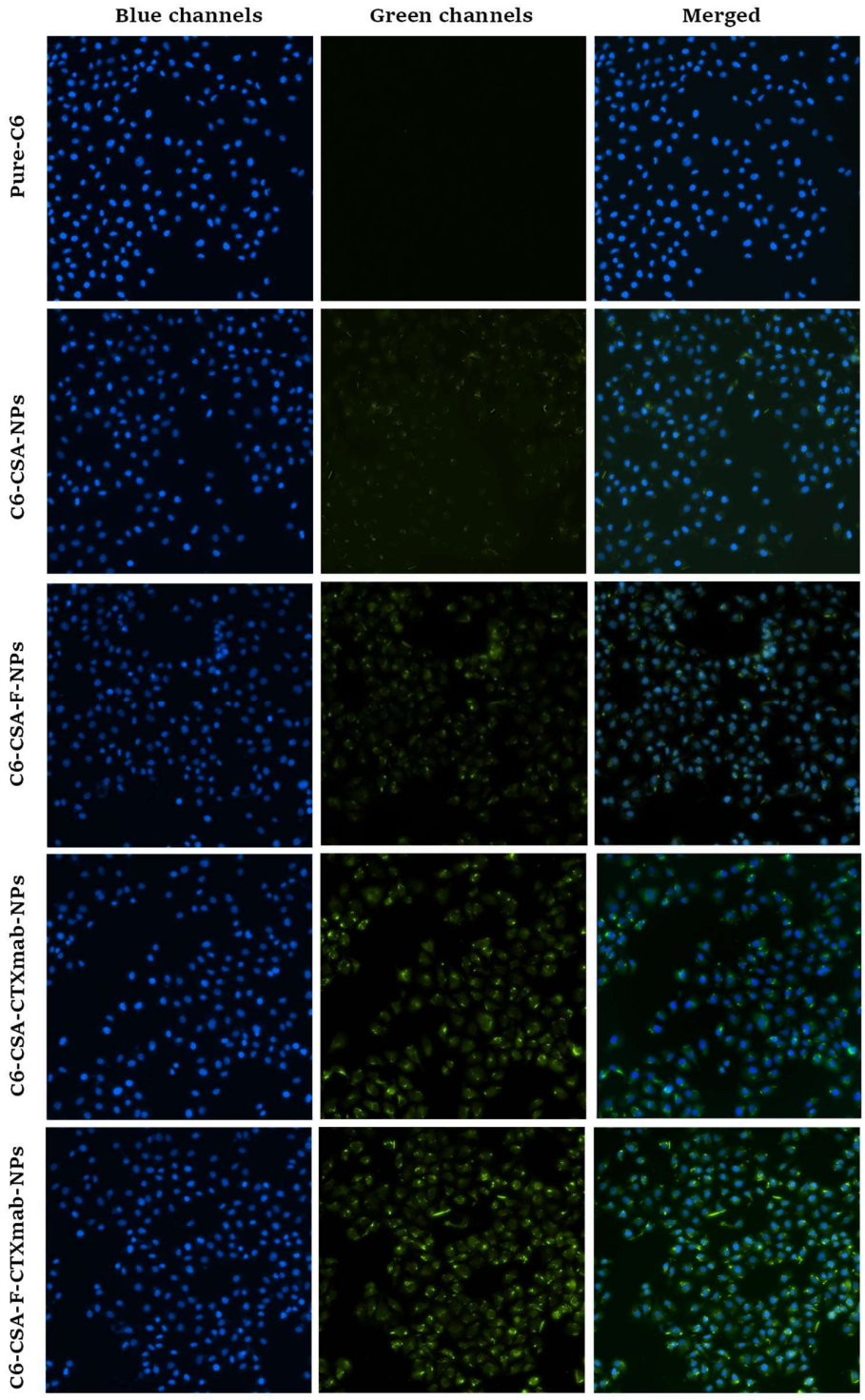

Figure 4.5. *In-vitro* cellular uptake study of pure C6 and C6-loaded CSA-NPs in A-549 cells

4.5.2.7.2. In-vitro cellular uptake study

Cellular uptake images of pure-C6 and C6-loaded CSA-NPs were captured for distinct green, blue, and a combination of both channels (**Figure 4.5**). The green channels represent the endocytosis of C6-loaded formulations, whilst the blue channels indicate the nucleus of the cells. The degree of cellular uptake was determined using image-J software by analysing the percentage of green channels. The percentage of green channels of pure C6, C6-CSA-NPs, C6-CSA-F-NPs, C6-CSA-CTXmab-NPs, C6-CSA-F-CTXmab-NPs was 0.38 ± 0.22%, 1.47± 0.23%, 14.76 ± 3.28%, 21.07 ± 2.24%, and 26.96 ± 1.51% respectively (**Figure 4.6 C**). The percentage of green channels of dual-receptor targeted CSA-NPs was significantly higher than pure-C6 ($p < 0.001$), non-targeted ($p < 0.001$), folate targeted ($p < 0.001$) and EGFR-targeted ($p < 0.05$) CSA-NPs. The substantial increase in cellular uptake of C6-CSA-F-CTXmab-NPs in A-549 cells can be possible because folate and EGF receptors exhibited a common endocytic pathway (via-caveolae) [189].

4.5.2.7.3. In-vitro cytotoxicity studies

The cytotoxicity of CZT, CZT-CSA-NPs, CZT-CSA-F-NPs, CZT-CSA-CTXmab-NPs and CZT-CSA-F-CTXmab-NPs was assessed by MTT assay against A-549 cells (human lung cancer cells) in comparison of SIRC cells (folate and EGFR negative cells). The previous studies have revealed that A-549 cells were overexpressed with EGFR and folate receptor-1 and can be used in the targeted drug delivery systems [128,208]. **Figure 4.6. A and 4.6. B** depict the percent cell viability of A-549 and SIRC cells after 24 h treatment with CZT control and CZT loaded CSA-NPs. The IC_{50} values of CZT control, CZT-CSA-NPs, CZT-CSA-F-NPs, CZT-CSA-CTXmab-NPs and CZT-CSA-F-CTXmab-NPs against A-549 cells was 15.27 ± 1.2, 8.11 ± 1.5, 6.49 ± 0.7, 5.33 ± 0.6 and 0.40 ± 0.03

µg/mL respectively. The non-targeted CZT loaded CSA-NPs showed the significant lower IC_{50} values than the CZT control ($p < 0.001$) due to their bioadhesion properties and the p-glycoprotein inhibitory effect of TPGS used in the formulation. The IC_{50} values of CZT-CSA-F-NPs, CZT-CSA-CTXmab-NPs, and CZT-CSA-F-CTXmab-NPs were significantly lower ($p < 0.05$, 0.01 and 0.001 respectively), as compared to CZT-CSA-NPs. The active targeted delivery of CZT-CSA-CTXmab-NPs and CZT-CSA-F-NPs via EGFR and folate-mediated endocytosis, possibly explains their higher cytotoxicity. Caveolae, the bulb-shaped plasma membrane invaginations, are involved in the common endocytic pathways of EGFR and folate receptors [209,210]. Therefore, the CSA-NPs targeted with dual-receptors showed the maximum cytotoxicity with the least IC_{50} values in A-549 cells ($p < 0.001$), demonstrating its enhanced synergistic uptake compared to non-targeted and single-receptor targeted CSA-NPs. Although, the results from the MTT assay performed on SIRC cells treated with CZT control, CZT-CSA-NPs, CZT-CSA-F-NPs, CZT-CSA-CTXmab-NPs and CZT-CSA-F-CTXmab-NPs showed the higher percentage of cell viability than A-549 cells. These results indicated that CZT-CSA-F-CTXmab-NPs may treat the lung cancer more efficiently, and therefore can reduce the dose-related side effects of CZT.

4.5.2.8. In-vivo evaluation

4.5.2.8.1. Pharmacokinetic study

The *in-vivo* pharmacokinetic assessment of CZT control and CZT loaded CSA-NPs was performed on Wistar rats by administrating intravenously at the equivalent dose of 3.5 mg/kg. Various pharmacokinetic metrics were computed (**Table 4.4.**) from the plasma CZT concentration and time profile. **Figure 4.7.** demonstrated the plasma CZT concentration and time profile of CZT control in contrast to CZT loaded CSA-NPs. The

clearance rate of CZT control is significantly higher ($p < 0.001$) than that of CZT-loaded CSA-NPs and therefore a frequent dosing is required to maintain a steady-state, which may result in significant adverse effects. The pharmacokinetic profile of CZT loaded nanoparticle formulations demonstrated an enhanced plasma half-life and mean residence time ($p < 0.001$) in contrast to CZT control.

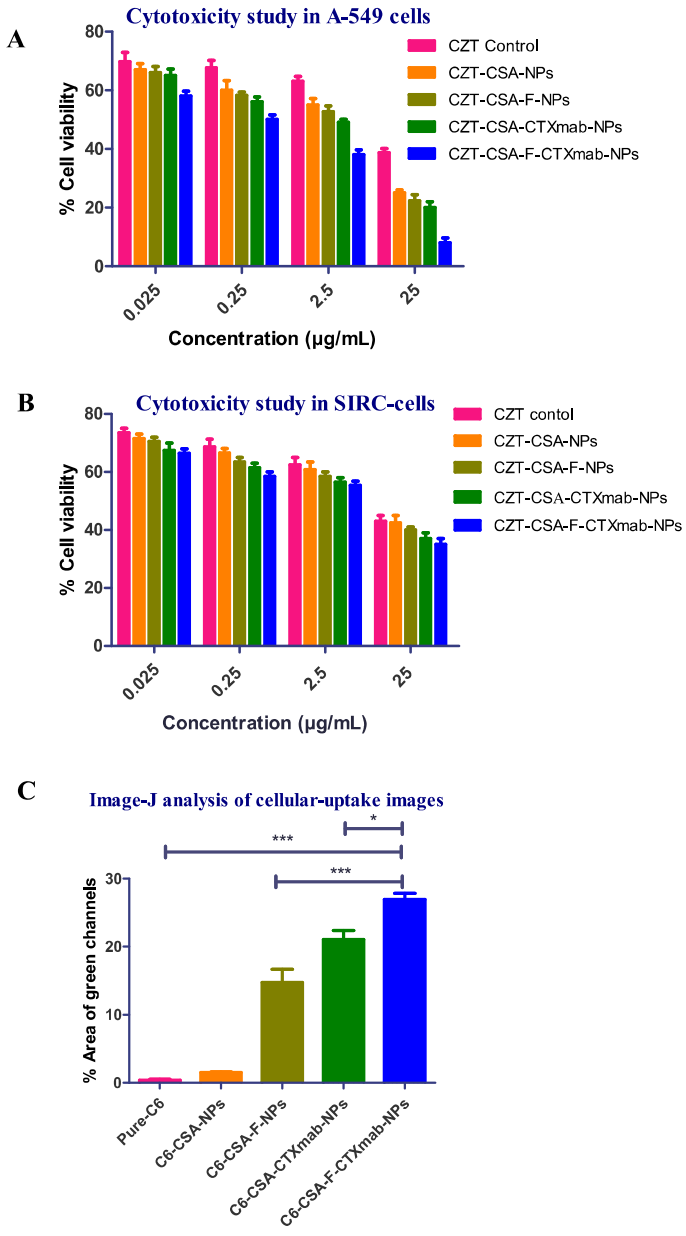

Figure 4.6. Cytotoxicity assessment of the CZT control and CZT loaded CSA-NPs against A) A-549 cells and B) SIRC cells, and C) histogram showing the percent area of green channels analyzed by Image-J software in respective cellular uptake images

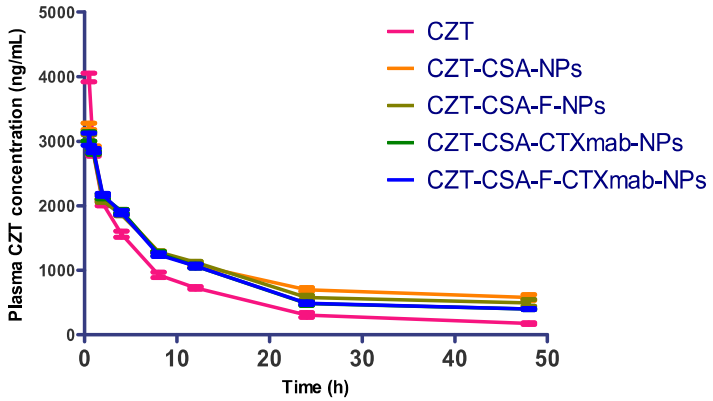

Figure 4.7. Plasma CZT concentration versus time profile

Table 4.4. Pharmacokinetic metrics of CZT control, CZT-CSA-NP, CZT-CSA-F-NP, CZT-CSA-CTXmab-NP, CZT-CSA-F-CTXmab-NP after i.v. injection at 3.5 mg/kg equivalent dose of CZT in Wistar rats

Pharmacokinetic metrics	CZT control (mean ± SD*)	CZT-CSA-NPs (mean ± SD*)	CZT-CSA-F-NPs (mean ± SD*)	CZT-CSA-CTXmab-NPs (mean ± SD*)	CZT-CSA-F-CTXmab-NPs (mean ± SD*)
AUC_{total} (ng.h/mL)	33675 ± 2061	61492 ± 2748	61294 ± 1947	58078 ± 2527	58801 ± 2224
C_{max} (ng/mL)	3988 ± 118	3141 ± 150	3074 ± 123	3022 ± 130	3032 ± 160
T_{max} (h) (extrapolated)	0	0	0	0	0
$T_{1/2}$(h)	18.6 ± 1.8	29.7 ± 3.3	27.7 ± 2.3	28.3 ± 2.1	28.53 ± 1.87
MRT(h)	20.8 ± 1.6	37.1 ± 4.7	36.9 ± 3.5	35.4 ± 2.4	35.28 ± 3.1
K_E (1/h)	0.041 ± 0.005	0.023 ± 0.008	0.020 ± 0.006	0.023 ± 0.003	0.024 ± 0.007
V_d (L/kg)	0.279 ± 0.007	0.257 ± 0.010	0. 238 ± 0.013	0.261 ± 0.027	0.243 ± 0035
CL_T (mL/kg.h)	10.44 ± 0.96	5.71 ± 0.62	5.14 ± 1.32	6.39 ± 0.11	5.98 ± 0.51
F_R	-	1.91 ± 0.35	1.82 ± 0.62	1.62 ± 0.030	1.74 ± 0.156

*n = 3
CZT-CSA-NPs: CZT loaded CSA-NPs
CZT-CSA-F-NPs: CZT loaded Folate targeted CSA-NPs
CZT-CSA-CTXmab-NPs: CZT loaded EGFR targeted CSA-NPs
CZT-CSA-CTXmab-F-NPs: CZT loaded dual receptor targeted CSA-NPs
AUC_{total}: Total area under the plasma CZT concentration curve
MRT: Mean residence time
V_d: Volume of distribution

CL_T: Total body clearance
K_E: Elimination rate constant
F_R: Relative bioavailability

4.5.2.8.2. Histopathological analysis

After repetitive administrations, the heart, lungs, liver, and kidneys of the animal group treated with the saline control revealed no pathological abnormalities (**Figure 4.8**). The animal group treated with CZT control had loosely organized cardiac fibres and massive hepatic necrosis. The CZT control (marketed formulation) consists of the tween-80 and ethanol for the solubilization, which might be responsible for the toxicity. Although the animals treated with CZT-CSA-NPs, CZT-CSA-F-NPs, CZT-CSA-CTXmab-NPs, and CTZ-CSA-F-CTXmab-NPs only exhibited partial lesions on histological examination. Consequently, when compared to a commercially available CZT formulation, the CSA-NPs were safer.

4.5.2.8.3. Tumour regression and survival analysis

Since tumour tissues have a higher cell count than normal cells, which is a distinguishable trait, as a result, assessing the cell number can reveal the extent of malignancy. Therefore, in this work, by determining the number of nuclei, the anticancer efficacy of all nanoparticle samples in contrast to the control group was analyzed **(Figure 4.9 A and 4.9 B)**. The number of nuclei in the microscopic images of the B(a)P treated group (cancer model control) was significantly higher ($p < 0.001$) than the control group. However, the number of nuclei in the microscopic images of the CZT-CSA-F-CTXmab-NPs treated group was significantly lower ($p < 0.001$) than in the cancer control group. Moreover, the dual receptor-targeted CSA-NPs treatment group also showed a substantially lower nucleus number than the folate and EGFR targeted formulations, indicating its synergic effect due to enhanced internalization in cancer cells. The Kaplan-Meier survival analysis **(Figure 4.9 C)** revealed the per cent survival of lung cancer induced mice treated with

CZT-CSA-F-CTXmab-NPs was significantly prolonged as compared to CZT control treated.

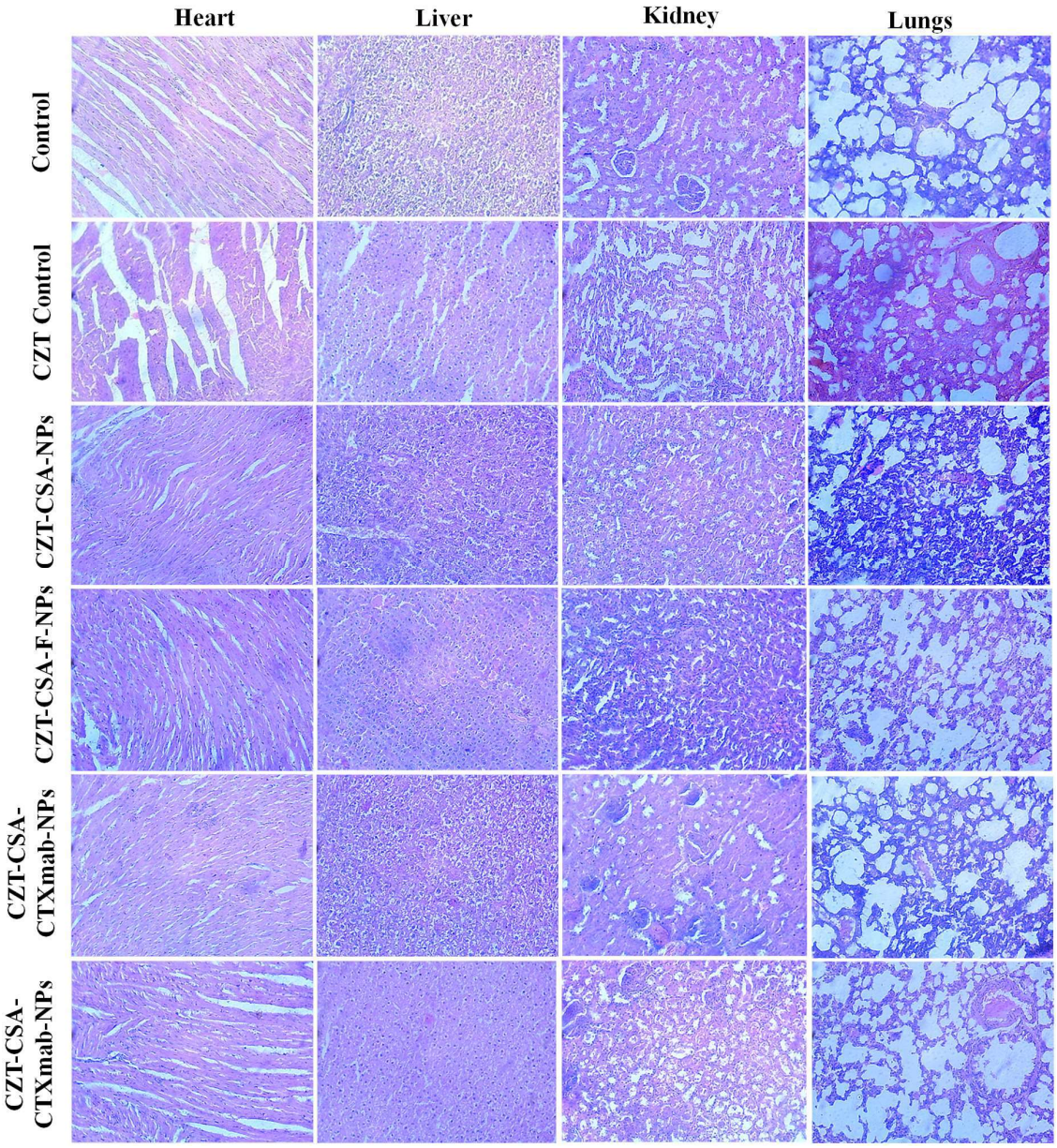

Figure 4.8. Histopathological assessment of the heart, liver, kidney and lungs of the Wistar rats treated with A) saline control, B) CZT-CSA-NPs, CZT-CSA-F-NPs, CZT-CSA-CTXmab-NPs and CZT-CSA-F-CTXmab-NPs

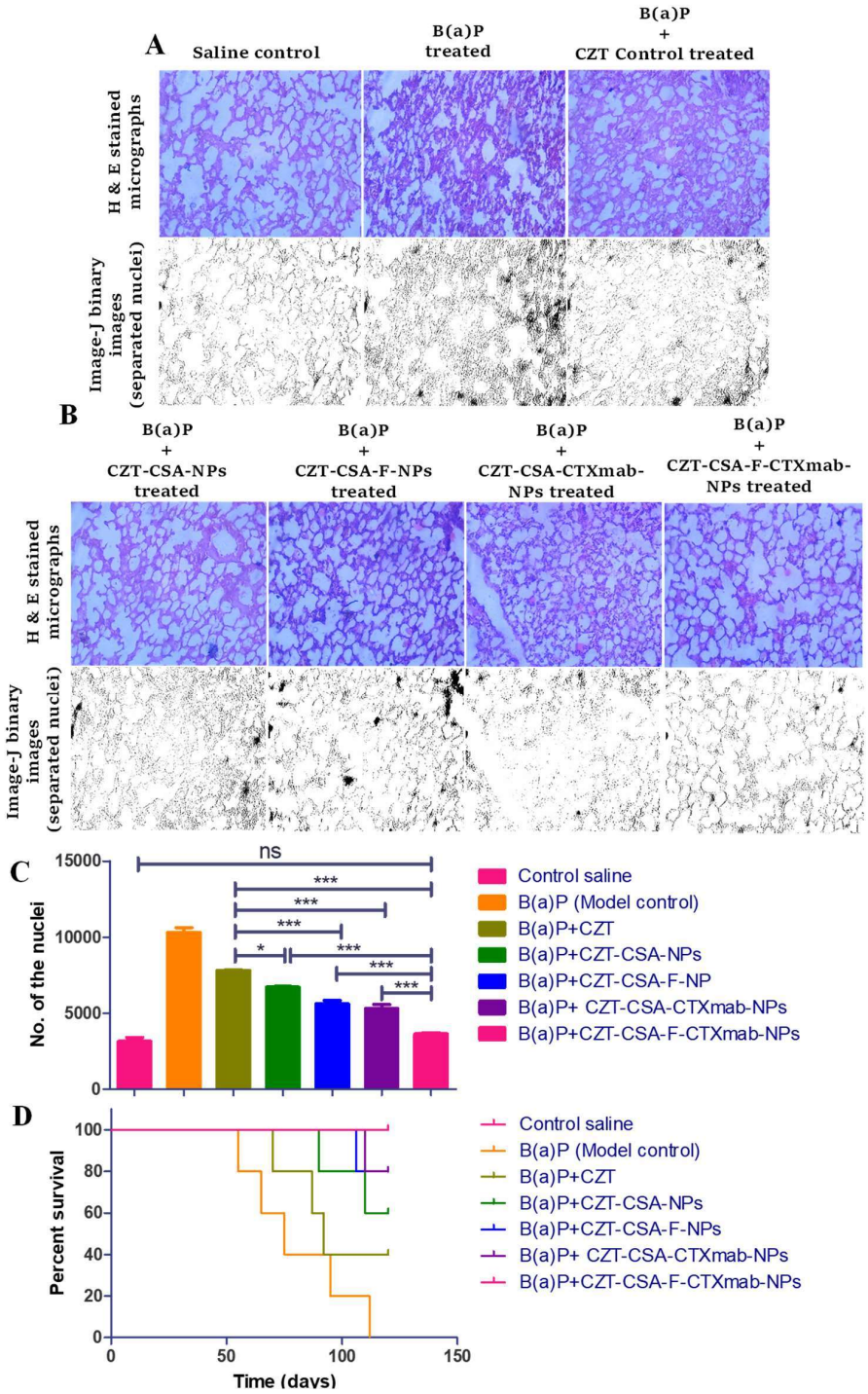

Figure 4.9. HE-stained micrograph and image-J processed binary B and W images of the separated blue channels of A) saline control, cancer model control, and CZT control-treated mice; B) CZT-CSA-NPs, CZT-CSA-F-NPs, CZT-CSA-CTXmab-NPs and CZT-CSA-F-CTXmab-NPs. C) number of the nucleus determined by analysing the corresponding B and W images of respective animal groups and D) Kaplan-Meier survival analysis of the corresponding groups of the mice up to 120 days

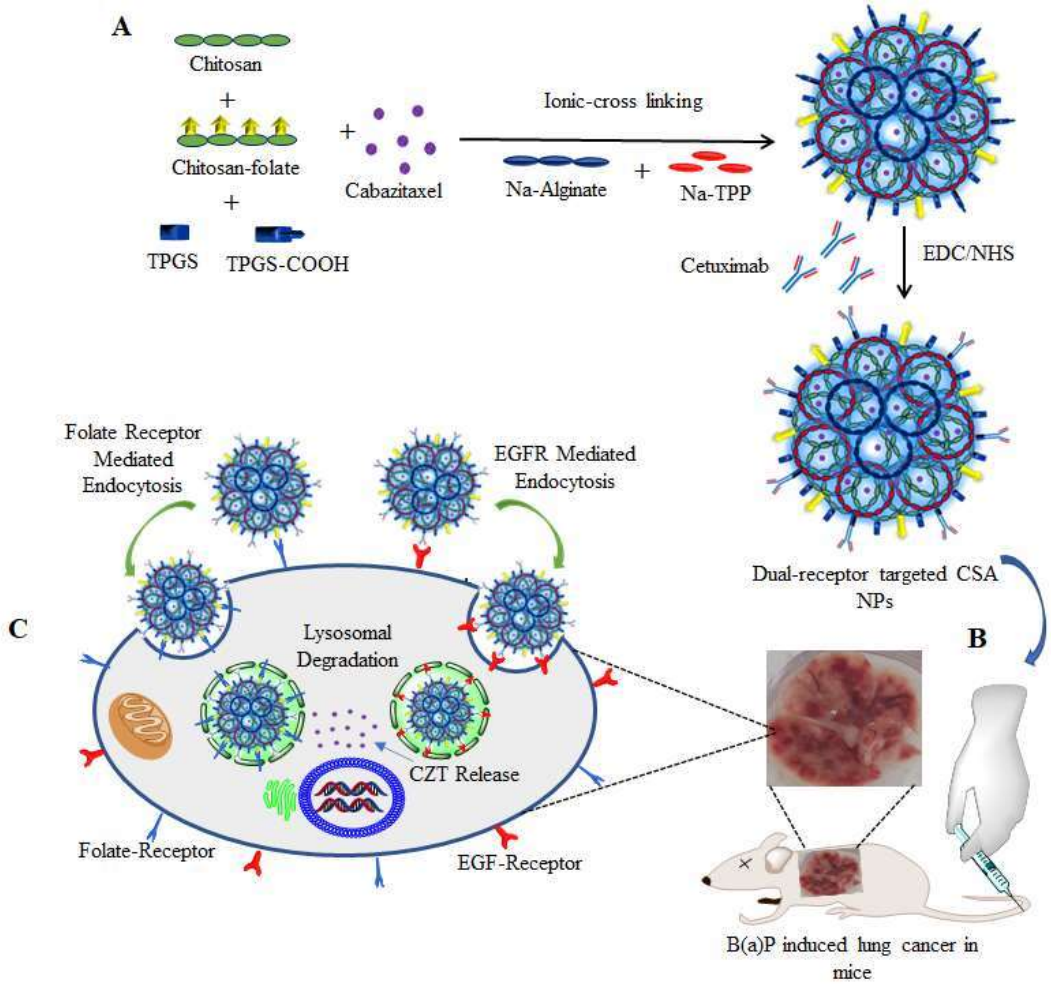

Figure 4.10. Graphical representation of the preparation of A) dual-receptor targeted CSA-NPs loaded with CZT and; B) showing the efficacy in B(a)P induced lung cancer mice and C) endocytosis mechanisms of nanoparticles in the lung cancer.

4.6. Conclusion

CSA nanoparticles targeting dual receptors were developed to efficiently treat the lung cancer. The combination of Na-TPP and Na-alginate was used as the crosslinking agents for the preparation of CSA-NPs. The dual-receptor targeted CSA-NPs were developed by utilizing the pre-conjugation technique for folic acid conjugation followed by the post-conjugation of CTXmab by using carbodiimide as cross-linkers (**Figure 4.10**). All the CSA nanoparticle formulations were analyzed through physicochemical parameters such as particle size, surface charge, SEM, TEM and AFM. Moreover, the *in-vitro* CZT

release, XRD analysis and surface chemistry of CSA-NPs were examined. The particle size, polydispersity and zeta potential of CSA-NPs were within the desired range. The surface charge of all the CSA-NPs ranged from to +25 mV to +32 mV, indicating that they were highly stable. The degree of folic acid and CTXmab conjugation was quantified by UV-Visible analysis and Bradford assay respectively.

Furthermore, XPS analysis also supports the successful conjugation of CTXmab and folic acid. The targeted CSA-NPs (single-receptor and dual-receptor targeted CSA-NPs) showed lower entrapment efficiency ($p < 0.05$) than non-targeted CSA-NPs. *In-vitro* release profiles revealed an initial burst release of CZT followed by the desired sustained release. The cellular-uptake study demonstrated that, dual-receptor targeted CSA-NPs internalized with higher extent in A-549 cells as compare to other CSA-NPs. The percentage of green channels of dual-receptor targeted CSA-NPs was significantly higher than pure-C6 ($p < 0.001$), non-targeted ($p < 0.001$), folate targeted ($p < 0.001$) and EGFR-targeted ($p < 0.05$) CSA-NPs. Moreover, the cytotoxicity study revealed that dual receptor-targeted CSA-NPs (CZT-CSA-F-CTXmab-NPs) showed the lowest IC_{50} (~38 folds) value against A-549 cells. The anticancer efficacy of the CZT loaded formulation was determined on the B(a)P induced lung cancer mice model, by analyzing the total number of nuclei of the HE-stained microscopic slides of each treatment group. As a result, when compared to other formulations, the dual-targeted CSA nanomedicine showed the highest anticancer activity and prolonged survival rate. Whereas, it exhibited better safety on Wistar rats. Hence, the outcomes of the proposed study have been proven to be adequate with a dual receptor targeting approach for advanced lung cancer treatment.